Density Functional Calculation of Structural and Vibrational Properties of Glycerol

Riccardo Chelli, Francesco L. Gervasio, Cristina Gellini, Piero Procacci, Gianni Cardini, and Vincenzo Schettino*

Università di Firenze, Dipartimento di Chimica, Via Gino Capponi 9, 50121 Firenze, Italy, and European Laboratory for Nonlinear Spectroscopy (LENS), Largo E. Fermi 2, 50125 Florence, Italy

Received: January 6, 2000; In Final Form: March 15, 2000

The conformational distribution of glycerol is still an open question both in gas and in liquid phase. Density functional calculations on different conformers of glycerol are reported and compared to the experimental infrared spectra of the gas and of the liquid. The experimental infrared spectra of gas and liquid glycerol are fitted by a linear combination of the single conformer ab initio spectra, obtaining the relative conformer concentrations. For the gas the results are in agreement with electron diffraction experiments and with molecular dynamics simulation data. The conformational distribution of glycerol in liquid phase is less accurate but always indicative. Some results about the role of the intramolecular hydrogen bonding in stabilization and in structural features of the conformers are discussed.

I. Introduction

Glycerol (1,2,3-propanetriol) has been the object of numerous investigations for its important role in biochemical reactions.[1] Glycerol, although being a molecule without asymmetric carbons, is metabolized asymmetrically.[1] This important property must be connected with conformational energetics that render the molecule prochiral.[1,2] The molecule is characterized by a high degree of flexibility and, due to the presence of three hydroxyl groups, can give rise to intra- and/or intermolecular hydrogen bonds (H-bonds). Each CH_2OH group can rotate around a CC covalent bond, giving three possible staggered conformations labeled by Bastiansen[3] as α, β, and γ. As illustrated in Figure 1, in the α conformation the end oxygen atom is in trans position with respect to the opposite end carbon; in the β conformation, the two oxygen atoms of the CH_2OH and CHOH groups are in trans position; finally, in the γ conformation the oxygen atom of the CH_2OH group is in trans position with respect to the aliphatic hydrogen atom of the CHOH group. Hence six different *backbone* structures, namely $\alpha\alpha$, $\alpha\beta$, $\alpha\gamma$, $\beta\beta$, $\beta\gamma$, and $\gamma\gamma$, can be identified irrespective of the hydroxyl hydrogen positions. Conformational distribution can be different for different aggregation states, due to the possibility to form intra- and intermolecular H-bonds. In fact, different conformers or mixtures of them have been identified or suggested as predominant in gas,[3,4] liquid,[5,6] and glassy[7] phases. The conformational structure of glycerol has been unambiguously identified only in the crystalline state, where X-ray diffraction[8] revealed the presence of only $\alpha\alpha$ backbone conformers. For all other phases, the available experimental and theoretical data are contradictory. Several ab initio studies[2,9,10] on the isolated molecule agree to indicate the $\gamma\gamma$ conformation as the most energetically stable implying, therefore, that in the gas phase glycerol exhibits mainly this conformation. These results seem to be confirmed by a recent experimental study where the gas phase rotational spectrum[4] of glycerol has been found consistent with a conformational distribution consisting in a mixture of $\gamma\gamma$ and, to a lower extent, of $\alpha\gamma$ forms. On the other hand, in a recent molecular dynamics (MD) simulation[11] of gaseous glycerol, the $\alpha\alpha$ and $\alpha\gamma$ structures were found as the most abundant in a wide temperature range (300−400 K). These last results were in agreement with electron diffraction experiments[3] which also indicated these backbone conformations as prevalent in the gas phase.

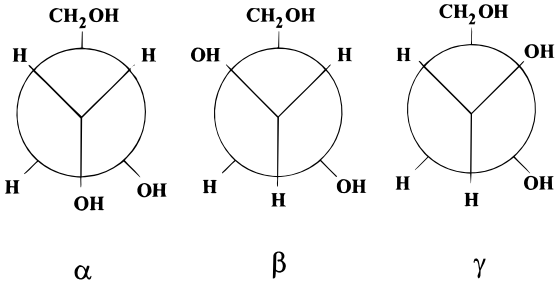

Figure 1. Newman projections of glycerol backbone conformations.

For the liquid and glassy states, available experimental studies have been unable to ascertain the conformational distribution. In two neutron scattering studies[5,6] the $\alpha\alpha$ and $\alpha\gamma$ conformations were invoked to explain the observed structure factors. This hypothesis has been later confirmed by MD simulations.[11,12] On the other hand, in a recent neutron scattering investigation,[7] the observed structure factors of glassy glycerol were fitted assuming a preferential conformational structure of $\beta\gamma$ type.

In order to shed further light on the structural properties of glycerol in gas and condensed phases, we have conducted a systematic correlated ab initio study of the vibrational properties of different glycerol structures, comparing the results with experimental data.[13,14] In the past, correlated ab initio calculations using the Møller−Plesset perturbation method (MP2) were performed by Teppen et al.[10] on 11 conformers, different in backbone conformation and hydroxyl group orientations. To our knowledge, however, no systematic and accurate ab initio study on the vibrational properties of glycerol is available in the literature. We have determined the vibrational frequencies along with the infrared (IR) and Raman intensities adopting density functional theory (DFT) at the B3-LYP/6-31G(d) level.[15−17] In

* To whom correspondence should be addressed. E-mail: schettin@chim.unifi.it.

10.1021/jp0000883 CCC: $19.00
Published on Web 05/11/2000

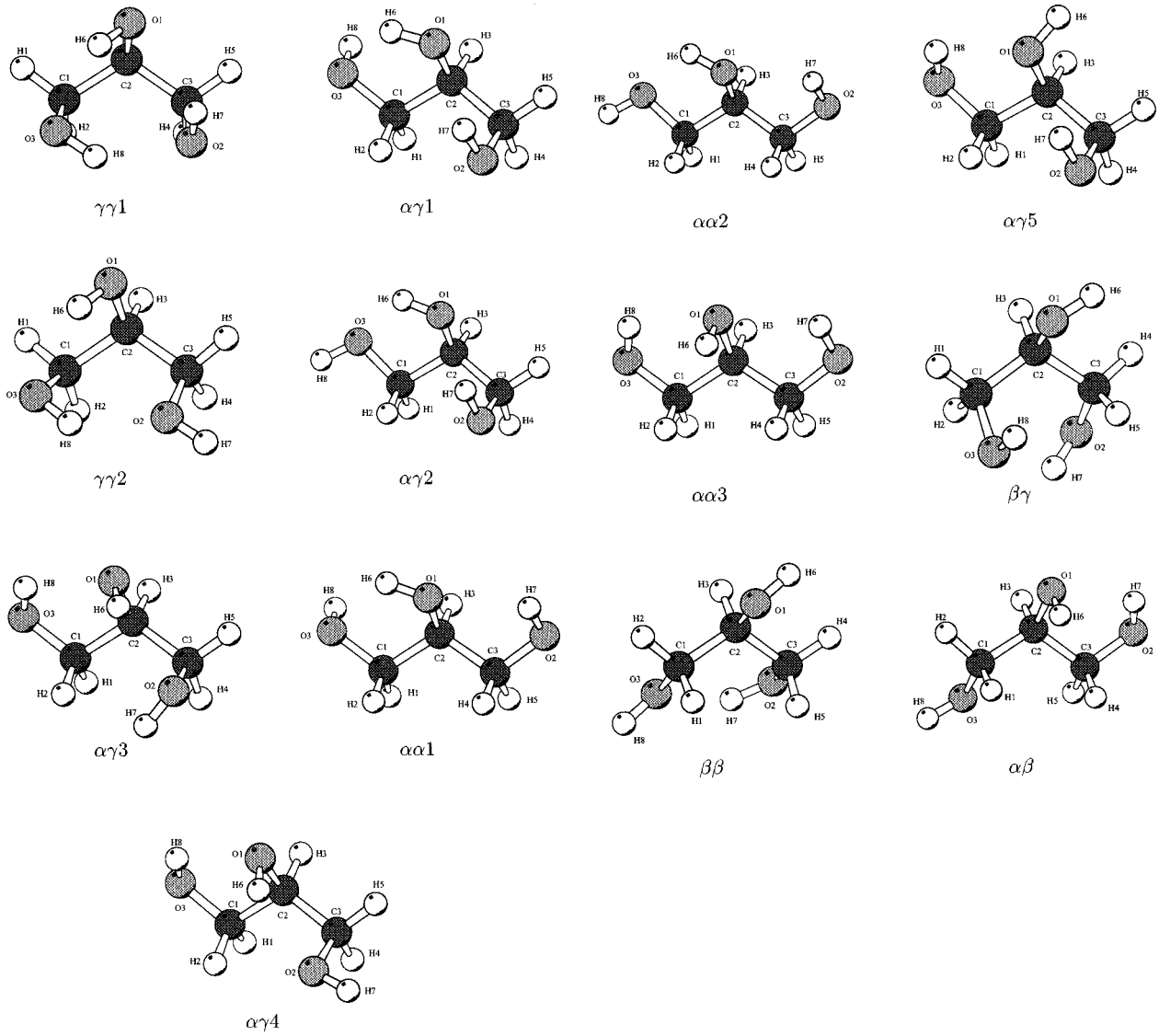

Figure 2. Computed structures of glycerol.

many cases[18−23] it was shown that this approach is able to accurately reproduce vibrational properties.

Ab initio computed spectra referring to monomer glycerol are here used to evaluate the conformational distribution in the gas phase by performing a fit of the experimental spectra. Furthermore, combined DFT data of monomers and dimers and experimental measurements can yield reliable indications on the conformational distribution of the liquid as well.

The layout of this paper is as follows: in section II some insights on the computational details are given. In section III structural features, related to H-bonding formation, are discussed. In the same section, the main results on the conformational distribution of glycerol in gas and liquid phases are given. Finally, conclusive remarks appear in section IV.

II. Calculations

As previously stated, the most stable backbone structures of glycerol in all phases involve the α and/or γ conformations. We have therefore chosen to study 10 different backbone conformers of αα, αγ, and $\gamma\gamma$ kind. The starting structures were taken from previous ab initio studies.[2,10] For completeness we have also included three structures involving the β conformation (αβ, $\beta\beta$, and $\beta\gamma$), for a total of 13 structures. The ab initio calculations have been performed using B3-LYP exchange-correlation functional,[15,16] as implemented in the Gaussian98 package.[24] Basis set selection is a key issue in our study because of the high computational cost required in the calculation of the IR and Raman spectra for many different minima. Based on our past experience,[19] we have used the standard split valence basis set 6-31G(d).[17] In fact, the combined use of this basis set and of the B3-LYP functional in DFT calculations has been proven[20,21] to provide an excellent compromise between accuracy and computational efficiency for large and medium-size molecules.

The coordinates of the optimized structures, their frequencies, and corresponding assignment along with IR and Raman intensities are available upon request to the authors.

III. Results and Discussion

A. Structural Properties. The optimized structures of the analyzed conformers are displayed in Figure 2 and labeled with two Greek letters that identify the backbone conformation followed by a number to discriminate, in order of increasing energy, among conformers having the same backbone arrangement and different OH orientations. The energies of the conformers are reported in Table 1 along with those obtained at the MP2 level by Teppen et al.[10] The energy ordering of the various conformations is not much different in the DFT and

TABLE 1: Energies of the Conformers shown in Figure 2[a]

conformer	E_{DFT}	ΔE_{DFT}	ΔE_{DFT+LJ}	ΔE_{MP2}
$\alpha\beta$	−344.762 528 122	26.30	23.097	
$\beta\beta$	−344.763 772 744	23.03	24.845	
$\beta\gamma$	−344.764 776 261	20.40	17.729	
$\alpha\alpha3$	−344.766 017 565	17.14	13.65	14.69
$\alpha\gamma5$	−344.766 864 349	14.92	11.629	10.59
$\alpha\alpha2$	−344.766 936 608	14.73	11.222	10.96
$\alpha\gamma4$	−344.767 346 228	13.65	10.498	9.54
$\alpha\alpha1$	−344.767 369 905	13.59	10.107	10.92
$\alpha\gamma3$	−344.767 650 937	12.85	9.266	11.55
$\alpha\gamma2$	−344.768 997 180	9.32	6.35	4.35
$\gamma\gamma2$	−344.769 149 872	8.91	12.456	6.40
$\alpha\gamma1$	−344.769 382 058	8.30	5.256	4.81
$\gamma\gamma1$	−344.772 544 584	0	0	0

[a] Entries in column 2 refer to absolute energies (atomic units) using DFT/B3-LYP method. Entries in columns 3 and 4 are the relative DFT/B3-LYP energies (kJ mol^{-1}) with respect to the most stable conformer ($\gamma\gamma1$) without (ΔE_{DFT}) or with (ΔE_{DFT+LJ}) Lennard-Jones corrections (see text), respectively. MP2 results (column 5) are taken from ref 10.

MP2 calculations. In fact, excluding conformers involving β arrangements, one can distinguish three subsets of conformations ($\alpha\gamma1$, $\gamma\gamma2$, $\alpha\gamma2$), ($\alpha\gamma3$, $\alpha\alpha1$, $\alpha\gamma4$, $\alpha\alpha2$, $\alpha\gamma5$), and ($\alpha\alpha3$) with very similar energy above the most stable $\gamma\gamma1$ conformer. The discrepancy is probably due to the absence of the dispersive contribution to the total energy in gradient-corrected DFT calculations.[25] In fact, the DFT energies have been corrected by adding an empirical Lennard-Jones atom−atom contribution based on the standard AMBER force field.[26] As can be seen from Table 1, for most of the conformers the energy difference between the MP2 and the Lennard-Jones corrected DFT values is within 1 or 2 kJ mol^{-1}, with the only exception of the $\gamma\gamma2$ conformer whose corrected energy is much too high. This conformer, however, is characterized by a very short O3−O2 distance (2.73 Å) and hence by a strongly repulsive Lennard-Jones (6.305 kJ mol^{-1}) contribution, very likely overcorrecting the corresponding DFT energy. In agreement with previous ab initio calculations,[9] the $\beta\beta$ conformer is found with an energy much higher than $\alpha\alpha$, $\gamma\gamma$, and $\alpha\gamma$ forms. A similar behavior was found for the $\alpha\beta$ and $\beta\gamma$ conformers. This fact is not surprising, as $\beta\gamma$, $\beta\beta$, and $\alpha\beta$, unlike all the others, have only one intramolecular H-bond as can be observed in Table 2 (we arbitrarily assume that an H-bond is established when the O···H distance is shorter than 2.5 Å).

In agreement with MP2 calculations,[10] the most stable conformer is $\gamma\gamma1$. This structure is characterized by the presence of three H-bonds, two of them being relatively strong with a H···O distance of 2.09 (H6···O3) and 2.05 Å (H8···O2), respectively (see Table 2). We note that the formation of the shortest H-bonds always occurs in conformers with a typical closed six-membered ring arrangement (−C−C−O···H−O−C−). In the $\gamma\gamma2$ and $\beta\beta$ conformers, for instance, the H8···O2 ($\gamma\gamma2$) and H7···O3 ($\beta\beta$) H-bonds, belonging to the six-membered ring −C2−C3−O2···H8−O3−C1− and −C2−C1−O3···H7−O2−C3−, have a length of 1.96 and 1.97 Å, respectively.

We observe in general that in all conformations the CO bond length markedly depends on the hydrogen donor (H-donor) or acceptor (H-acceptor) character of the oxygen atom. The C3−O2 average distance is, e.g., about 1.416 Å when O2 is H-donor ($\alpha\alpha1$, $\alpha\alpha2$, $\alpha\alpha3$, $\alpha\gamma1$, $\alpha\gamma2$, and $\alpha\gamma5$), while it increases to 1.433 Å when O2 behaves as H-acceptor ($\gamma\gamma2$, $\alpha\gamma3$, and $\alpha\gamma4$). When the oxygen is H-acceptor as well as H-donor (for instance O1 in the $\gamma\gamma1$, $\alpha\gamma1$, $\alpha\gamma2$, $\alpha\gamma3$, $\alpha\alpha1$, $\alpha\gamma4$, and $\alpha\alpha2$ conformers), the H-acceptor effect is dominating and the CO bond length increases on average to 1.427 Å. In fact, in the $\alpha\beta$ conformer, where the H8−O3 hydroxyl group is not involved in H-bonding, the C1−O3 covalent bond is 1.4207 Å.

TABLE 2: H-Bond Distances (Å) and H-Bond Angles (deg) of Glycerol Conformers[a]

	$\alpha\alpha1$	$\alpha\alpha2$	$\alpha\alpha3$	$\gamma\gamma1$	$\gamma\gamma2$
H6···O3	2.1911	2.2235		2.0893	2.1215
H6···O3−H8	105.76	135.55		94.82	92.69
H8···O1			2.2625		
H8···O1−H6			98.00		
H8···O2				2.0533	1.9639
H8···O2−H7				93.29	141.97
H7···O1	2.2590	2.2355	2.2625	2.4007	
H7···O1−H6	166.29	156.68	98.00	81.17	

	$\alpha\gamma1$	$\alpha\gamma2$	$\alpha\gamma3$	$\alpha\gamma4$	$\alpha\gamma5$
H6···O3	2.1013	2.0975			
H6···O3−H8	105.42	131.29			
H6···O2			2.1454	2.1609	
H6···O2−H7			108.68	134.46	
H8···O1			2.1521	2.1938	2.2595
H8···O1−H6			116.94	112.66	127.48
H7···O1	2.2298	2.2226			2.2479
H7···O1−H6	124.89	131.09			111.40

	$\alpha\beta$	$\beta\beta$	$\beta\gamma$
H7···O1	2.2381		
H7···O1−H6	100.53		
H7···O3		1.9733	2.4693
H7···O3−H8		132.88	124.07

[a] H-bond distances greater than 2.5 Å are not reported. Atomic symbols refer to Figure 2.

From Tables 1 and 2, we can observe that the energetically favored $\gamma\gamma$ and $\alpha\gamma$ conformations are often characterized by strong (i.e., short) H-bonds. However, the H-bond length is not the only driving factor for energy stabilization: the $\alpha\gamma2$ conformer is less stable than $\alpha\gamma1$, despite the fact that its H-bonds (H6···O3 and H7···O1) are shorter and hence presumably stronger than in $\alpha\gamma1$. From the analysis of the optimized structures it emerges that an important structural feature for energy stabilization in intramolecular H-bonding is the orientation of the lone pair of the H-acceptor oxygen. For example, in the most stable $\alpha\gamma$ conformer ($\alpha\gamma1$) the H6···O3−H8 angle is 105.4° (very close to the ideal sp^3 hybridization value), which means that H6 is pointing toward the O3 lone pair. In $\alpha\gamma2$ the short O3···H6 H-bond forms an angle of 131.3° with the O3−H8 bond, missing by more than 20° the lone pair.

It is indeed remarkable that the most stable backbone conformer of $\alpha\alpha$ type, i.e., $\alpha\alpha1$, has a relatively high energy. We recall that crystalline glycerol is made exclusively by $\alpha\alpha$ conformers and in the liquid and glassy phases the $\alpha\alpha$ conformation, together with the $\alpha\gamma$, is believed[5,6,11] predominant. The energy stabilization of $\alpha\alpha$ conformers (as well as $\alpha\gamma$) in the condensed phases should be attributed to the formation of intermolecular H-bonds.[5,6] This is certainly true in the crystal phase where each glycerol molecule is involved in six intermolecular H-bonds, with three oxygen atoms acting as H-donors and three as H-acceptors.[12] In liquid and glassy glycerol, the stabilization of the $\alpha\alpha$ form has probably a more subtle origin with entropic factors, along with intermolecular interactions, also playing an important role.[11]

B. Vibrational Spectra. *1. Gas Phase.* As stated in the Introduction, there is no agreement on the conformational distribution in the gas phase. Comparison of the gas phase experimental IR spectrum of glycerol[14] to the calculated individual spectra of the various conformers may be of great help in resolving the matter of the conformational composition

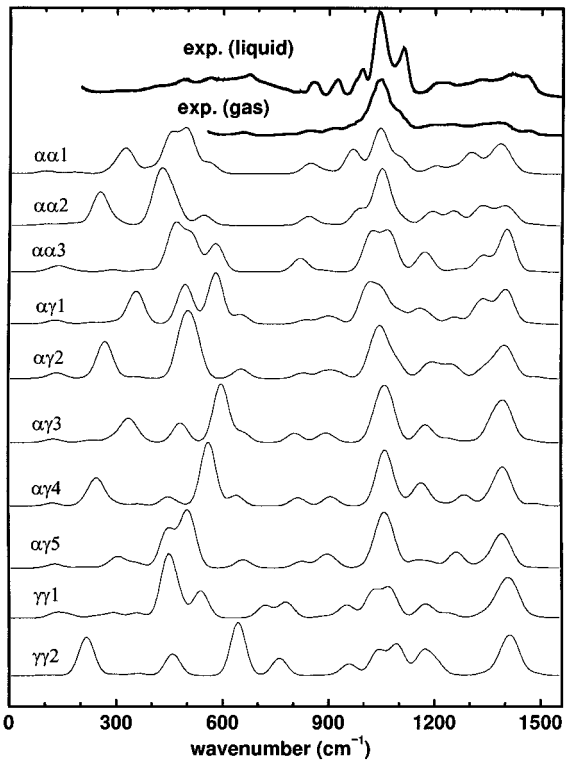

Figure 3. Calculated IR spectra of monomers (see text for details) compared to the experimental gas phase IR spectrum[14] at 498 K, and to the measured liquid phase spectrum at room temperature. The IR spectrum of the liquid was measured by means of a FTIR Bruker interferometer IFS-120 with a spectral resolution of 2 cm^{-1}. Liquid glycerol (purity greater than 99.5%) was furnished by Fluka Chemie (Switzerland). The bandwidth of the calculated spectra is 50 cm^{-1}.

in the gas phase. To this aim, we have computed the vibrational frequencies along with IR and Raman intensities for the conformers of $\alpha\alpha$, $\alpha\gamma$, and $\gamma\gamma$ types (the Raman intensities have been computed only for $\alpha\alpha1$, $\alpha\alpha2$, $\alpha\gamma1$, $\alpha\gamma2$, $\gamma\gamma1$, and $\gamma\gamma2$ conformers). In our analysis we have not considered conformers with β conformation because of their very high energy (see Table 1) and since no experimental evidence of their presence in gas phase was found in the past.[3,4]

The theoretical spectra are obtained by representing each band with a Gaussian profile, centered at the calculated frequency and with intensity equal to the corresponding calculated intensity. In Figure 3 we report the ab initio IR spectra for the analyzed conformers compared to the experiments in the gas and liquid phases at 498 K and room temperature, respectively. The gas phase IR spectrum was taken from ref 14, while that of the liquid was obtained in this work (see caption of Figure 3 for experimental details). Unfortunately, the Raman spectrum of the gas phase is not available, and therefore, we shall only discuss the IR spectrum.

From the knowledge of the ab initio spectra of the individual conformers, one can deduce the conformational distribution in the gas by fitting the experimental spectra with a *linear* combination of the individual spectra, the coefficients of the linear combination yielding the conformational distribution. The success of the procedure relies on a reasonable accuracy of the DFT-calculated IR frequencies and intensities[19,23] and on the availability of a selective spectral region for discerning among the various conformers.

From a qualitative comparison of the experimental spectrum with ab initio calculated spectra of the various conformers (Figure 3), one could argue that the 550−1600 cm^{-1} region has indeed the desired selectivity. In fact, it can be seen from Figure 3 that the $\gamma\gamma$ conformations exhibit the highest intensity at ∼1400 cm^{-1} (COH bending motion) while for $\alpha\alpha$-type structures the strongest bands are expected at ∼1050 cm^{-1} (CO stretching modes). The CCC backbone symmetric stretching mode at ∼850 cm^{-1} gives a significant intensity only in the $\alpha\alpha$ and, to a lower extent, the $\alpha\gamma$ conformers. On the contrary, the high-frequency region of CH and OH modes is not so useful for our purposes since anharmonic effects, not included in the DFT calculation, are expected to be important for these modes.

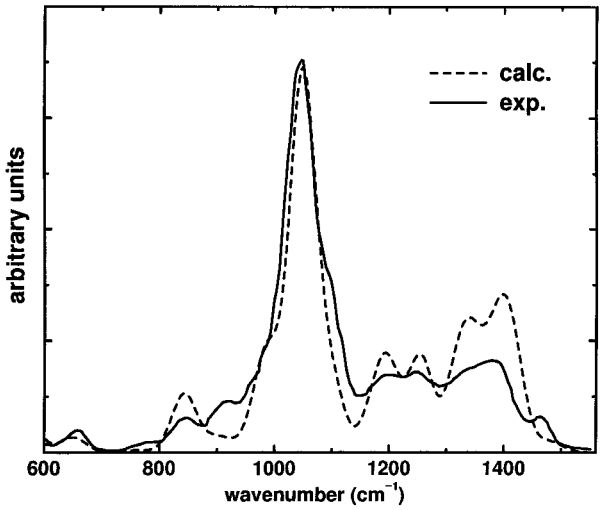

Figure 4. Best fit to the experimental gas phase IR spectrum of glycerol (see text for details). Full line, experimental; dashed line, calculated.

On the basis of the above consideration and of a first sight comparison of observed and calculated spectra, one could infer that the $\gamma\gamma$ conformers should only be a minor contributor of the conformational mixture in the gas phase compared to more abundant $\alpha\alpha$ and $\alpha\gamma$ conformers. To put these considerations in a quantitative assessment, the glycerol gas phase spectrum has been calculated as an overlap of the monomer spectra

$$S_{\mathrm{calc}}(\omega) = \sum_i \sum_j C_j I(\omega_{ij})\, \mathrm{e}^{-(\omega-\omega_{ij})^2/w^2} \qquad (3.1)$$

where i and j label the normal modes and the conformers, respectively, ω_{ij} and $I(\omega_{ij})$ are the calculated frequencies and intensities, C_j is the fractional concentration of the jth conformer, and W (common to all the conformers) is related to the band width Γ by the relation $\Gamma = 2W\sqrt{\ln 2}$. The fit to experiments of the calculated spectrum (3.1) has been estimated through the quantity[27]

$$F = \frac{\int_{\omega_{\min}}^{\omega_{\max}} S_{\mathrm{exp}}(\omega)\, S_{\mathrm{calc}}(\omega)\, \mathrm{d}\omega}{\left[\int_{\omega_{\min}}^{\omega_{\max}} S_{\mathrm{exp}}{}^2(\omega)\, \mathrm{d}\omega \int_{\omega_{\min}}^{\omega_{\max}} S_{\mathrm{calc}}{}^2(\omega)\, \mathrm{d}\omega\right]^{1/2}} \qquad (3.2)$$

The parameter 3.2 will range from 1, when the two spectra are identical, to 0, when there is no overlap between the two spectra. By minimizing the function $g = 1 - F$ with respect to the adjustable parameters C_j (W was fixed to 30 cm^{-1}) and using $\omega_{\min} = 550$ cm^{-1}and $\omega_{\max} = 1600$ cm^{-1}, we obtained the best fit to the observed IR spectrum ($F = 0.96$) shown in Figure 4. The obtained parameters were $C_{\alpha\alpha} = 0.83$, $C_{\alpha\gamma} = 0.15$, and $C_{\gamma\gamma} = 0.02$. The agreement with experiments is satisfactory, and the fit gives the conformational composition at the temperature of the experiment, i.e., 498 K.

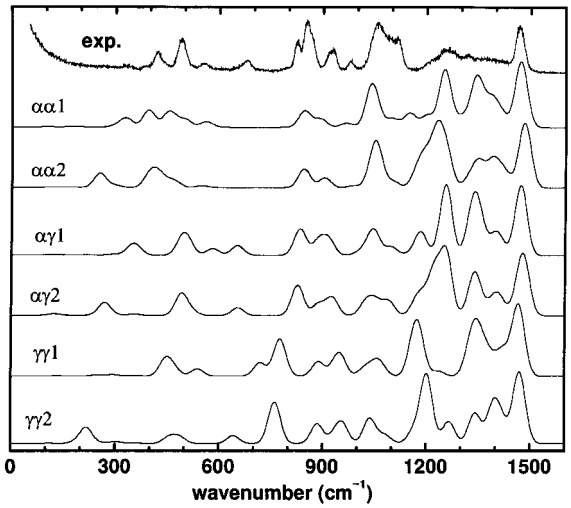

Figure 5. Calculated Raman spectra of monomers (see text for details) compared to the experimental Raman spectrum of liquid glycerol, measured using the 514.5 nm line of an Ar^+ laser with resolution 2 cm^{-1}.

Our results are consistent with indications from MD simulation of gas glycerol[11] and agree with previous electron diffraction studies.[3] Since the IR spectrum of the liquid, recorded at 300 K, has many similarities with the experimental gas spectrum in the 750−1600 cm^{-1} region, the conformational composition should not vary dramatically with temperature in the range 300−500 K in going from the gas to the liquid phase.

2. Liquid Phase. Both the IR and Raman spectra of liquid glycerol are available. The Raman spectrum has been obtained in this work and is shown in Figure 5 (see caption to figure for experimental details) compared with the ab initio calculated spectra of some conformers.

Derivation of the conformational distribution in the liquid phase using the same procedure as in the gas phase poses some problems. In fact, in the gas phase it could safely be assumed that the experimental spectrum was the superposition of contributions from spectra of the various conformers since formation of associated species (dimers, trimers, etc.) is unlikely in the gas. On the contrary, in the liquid one should expect strong intermolecular H-bonds are formed which are associated with novel intermolecular bands and with significant shift or increased intensities of the fundamentals. These effects are more likely to occur in the low-frequency region of the spectrum ($\omega < 700$ cm^{-1}) and in the OH stretching region.

For these reasons, before proceeding to a fit of the liquid spectra, we decided to verify the actual effect of intermolecular association to the vibrational spectra. For this purpose the ab initio IR and Raman spectra of αα···αα, αα···αγ, and αγ···αγ dimers were calculated optimizing the structures of the dimers to allow for a distortion of αα1, αα2, αγ1, and αγ2 monomers. In the dimers multiple and strong intermolecular H-bonds are formed (three H-bonds for each dimer) with O···H bond distance ranging from 1.76 to 1.94 Å. In Figures 6 and 7 the dimer spectra are compared with the sum spectra of the monomer partners. From the figures it can be seen that both in the low-frequency region and in the OH stretching region the dimer spectrum drastically differs from the monomer sum spectrum. This is most clearly evident from the low values of the *F* factor calculated according to eq 3.2. It is therefore evident that these spectral regions are not suitable for a fit of the liquid spectrum in terms of monomers' contributions. However, it can also be seen from Figures 6 and 7 that in the 750−1500 cm^{-1} frequency region the association effect in the dimers is not much pronounced and, in fact, the *F* factor is higher than 0.89. Therefore, this spectral region can be confidently used also in the liquid phase to sort out a conformational distribution from a fit of the observed spectra to a superposition of monomer spectra. We consider this to be reliable at a semiquantitative level in view of the fact that the association effects on the

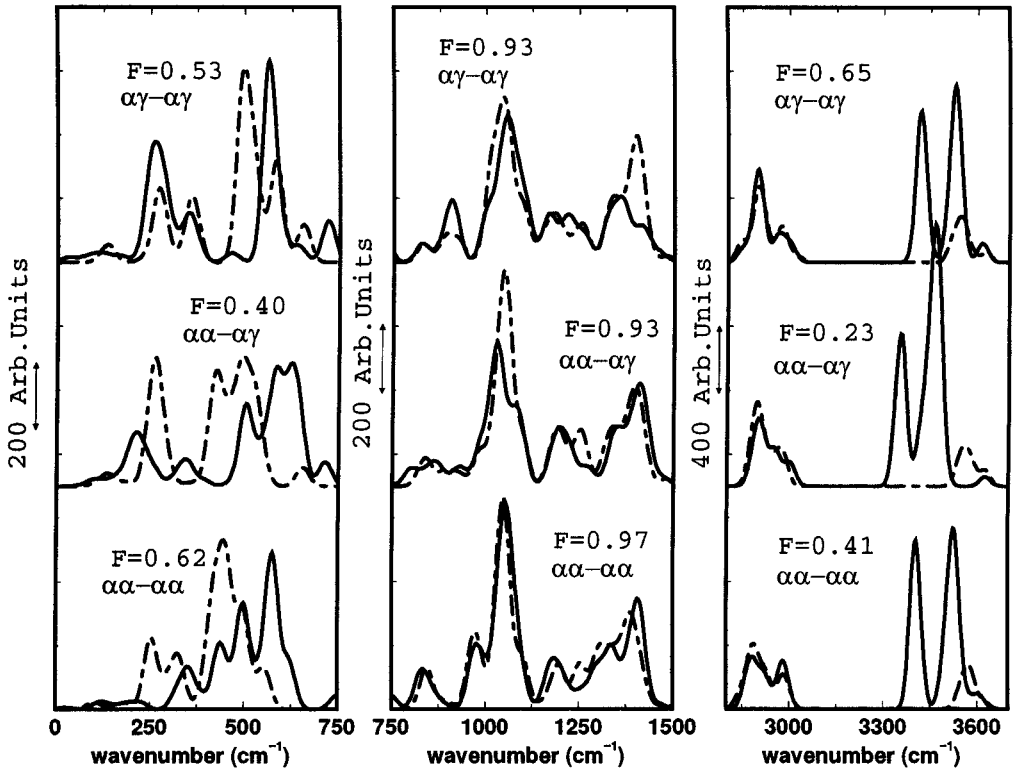

Figure 6. Calculated IR spectra of the dimers (full line) and sum spectra of the corresponding partners (dashed line). The *F* factors are defined in eq 3.2.

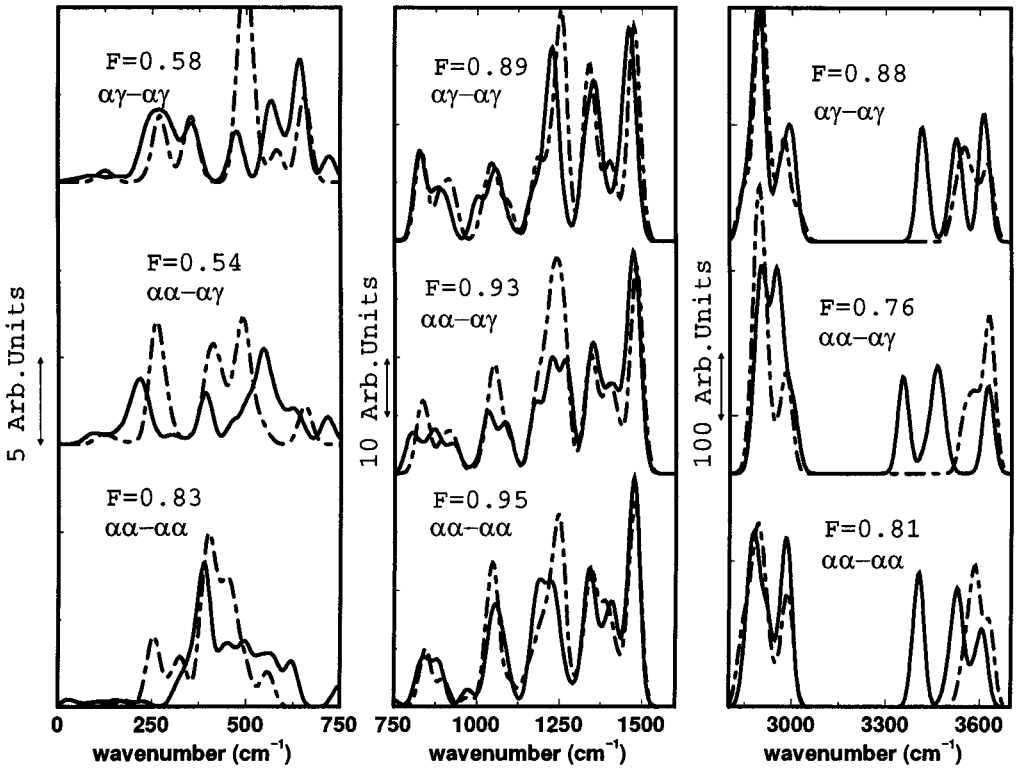

Figure 7. Calculated Raman spectra of the dimers (full line) and sum spectra of the corresponding partners (dashed line). The *F* factors are defined in eq 3.2.

spectra, certainly important in the liquid state, can only be crudely evaluated by our calculation on tightly H-bonded dimers.

By using the same procedure as in the gas phase, a single and well-defined global minimum was obtained for the C_j parameters (see eq 3.1) from the IR spectrum. By contrast, the fit of the Raman spectrum yielded multiple and high valued minima for the *g* function with disparate and unreliable values of the C_j coefficient. The failure of the fitting procedure in the case of the Raman spectrum can be due mainly to a poor reliability of the calculated Raman intensities. In fact, it is now well established[28] that electronic polarizability is very sensitive to the basis set size and therefore the 6-31G* basis set may not be entirely reliable for predicting Raman activity.

The best fit of the IR spectrum yields $F = 0.938$ (eq 3.2), a value slightly lower than in the gas phase. The resulting fractional concentrations are $C_{\alpha\alpha} = 0.74$, $C_{\alpha\gamma} = 0.07$, and $C_{\gamma\gamma} = 0.19$ (with $W = 30.0$ cm^{-1}). We remark that the $\gamma\gamma$ contribution is entirely given by the $\gamma\gamma 2$ form. This form in the calculated monomer IR spectrum shows a well-defined absorption band at about 650 cm^{-1} that does not seem to have a counterpart in the experimental spectrum. Furthermore, the presence of a significant quantity of $\gamma\gamma$ in the liquid is unlikely from both theoretical[11] and experimental indications.[5,6] If we perform the fit by arbitrarily excluding the $\gamma\gamma 2$ conformer from eq 3.1, we find a result similar to that found in the gas phase, i.e., $F = 0.93$, $C_{\alpha\alpha} = 0.70$, $C_{\alpha\gamma} = 0.27$, and $C_{\gamma\gamma} = 0.03$. Such a result is in agreement with MD simulations[11] on liquid glycerol.

It can therefore be concluded that on the basis of DFT calculations, even if quantitative conclusions on the conformational composition of the liquid glycerol cannot be drawn, the liquid composition should be similar to that in the gas phase and in particular that αα conformer is the more abundant.

IV. Conclusions

We have performed ab initio calculations of the structural and vibrational properties of glycerol in order to obtain information on the conformational equilibria in the gas and liquid phases. By comparing calculated intensities to available experimental data, we have gathered convincing evidence that gaseous glycerol basically exists in two forms, the αα and the $\alpha\gamma$ structures, and all other forms, including the very stable $\gamma\gamma$ form, have a negligible concentration. The strong similarity of the experimental spectra of the gas and of the liquid in the 750−1600 cm^{-1} spectral region implies that the conformational composition of the liquid is similar to that of the gas phase. As there is widespread agreement in the literature on the fact that in condensed phase the αα form is prevalent, the similarity of the gas and liquid IR spectra can be used as further evidence of the existence of the αα form in the gas phase. Our combined ab initio and experimental approach confirms the prediction of a recent MD investigation on glycerol,[11,12] where conformational distribution of the gas and liquid phases were found to be very similar and weakly dependent on temperature in the range 300−400 K and consisting mainly of αα and $\alpha\gamma$ conformers. Our results are also in agreement with earlier electron diffraction studies on the gas phase[3] of glycerol and on more recent neutron scattering measurements in liquid phase.[5,6]

It seems that these conclusions are not in agreement with the rotational spectrum obtained by Maccaferri et al.[4] on free jet expanded glycerol, which could be interpreted considering that only the $\gamma\gamma$ and $\alpha\gamma$ conformers are present in the gaseous sample. In the assumption that the conformational distribution at the temperature of the preexpanded gas (423 K) is fully quenched during the expansion, the αα conformer should be revealed in the rotational spectrum, since its dipole moment is similar in magnitude to those of $\gamma\gamma$ and $\alpha\gamma$, and the rotational constants of the various conformers differ appreciably (as is reported in the additional material available from the authors).

However, it is well-known[29,30] that when the interconversion energy barriers are low, as it is the case for glycerol,[11] a structural relaxation occurs during the expansion. This relaxation can be particularly effective if argon is the carrier gas as in the experiment by Maccaferri et al.[4] If this is the case, the difference from Maccaferri's results can be explained.

Acknowledgment. This work was supported by the Italian Ministero dell'Università e della Ricerca Scientifica e Tecnologica (MURST), by the Consiglio Nazionale delle Ricerche (CNR), and by the European Union (Contract No. ERBFMGECT950017). We are grateful to Piero R. Salvi and Giuseppe Sbrana for their useful suggestions and Sonia Melandri and Walther Caminati for interesting discussions.

References and Notes

(1) Blackmore, P. F.; Williams, J. F.; Clark, M. G. *J. Chem. Educ.* **1973**, *50*, 555.

(2) van Den Enden, L.; van Alsenoy, C.; Scarsdale, J. N.; Schäfer, L. *J. Mol. Struct. (THEOCHEM)* **1983**, *104*, 471.

(3) Bastiansen, O. *Acta Chem. Scand.* **1949**, *3*, 415.

(4) Maccaferri, G.; Caminati, W.; Favero, P. G. *J. Chem. Soc., Faraday Trans.* **1997**, *93*, 4115.

(5) Champeney, D. C.; Joarder, R. N.; Dore, J. C. *Mol. Phys.* **1986**, *58*, 337.

(6) Garawi, M.; Dore, J. C.; Champeney, D. C. *Mol. Phys.* **1987**, *62*, 475.

(7) Dawidowski, J.; Bermejo, F. J.; Fayos, R.; Perea, R. F.; Bennington, S. M.; Criado, A. *Phys. Rev. E* **1996**, *53*, 5079.

(8) van Koningsveld, H. *Recl. Trav. Chim.* **1968**, *87*, 243.

(9) van Alsenoy, C.; Klimkowski, V. J.; Ewbank, J. D.; Schäfer, L. *J. Mol. Struct. (THEOCHEM)* **1985**, *121*, 153.

(10) Teppen, B. J.; Cao, M.; Frey, R. F.; van Alsenoy, C.; Miller, D. M.; Schäfer, L. *J. Mol. Struct. (THEOCHEM)* **1994**, *314*, 169.

(11) Chelli, R.; Procacci, P.; Cardini, G.; Califano, S. *Phys. Chem. Chem. Phys.* **1999**, *1*, 879.

(12) Chelli, R.; Procacci, P.; Cardini, G.; Valle, R. G. D.; Califano, S. *Phys. Chem. Chem. Phys.* **1999**, *1*, 871.

(13) Beaudoin, J.-L.; Manisse, A.; Benchenane, A.; Harrand, M. *C. R. Acad. Sci.* **1971**, *273B*, 15.

(14) NIST Mass Spec Data Center, S. E. Stein, Director; IR and Mass Spectra. In *NIST Chemistry WebBook*, NIST Standard Reference Database Number 69; Mallard, W. G., Linstrom, P. J., Eds.; National Institute of Standards and Technology: Gaithersburg, MD, November 1998; http://webbook.nist.gov.

(15) Becke, A. D. *Phys. Rev. A* **1988**, *33*, 3098.

(16) Lee, C.; Yang, W.; Parr, R. G. *Phys. Rev. B* **1988**, *37*, 785.

(17) Hariharan, P. C.; Pople, J. A. *Theor. Chem. Acta* **1973**, *28*, 213.

(18) Schettino, V.; Gervasio, F. L.; Cardini, G.; Salvi, P. R. *J. Chem. Phys.* **1999**, *110*, 3241.

(19) Gervasio, F. L.; Cardini, G.; Salvi, P. R.; Schettino, V. *J. Phys. Chem. A* **1998**, *102*, 2131.

(20) Rauhut, G.; Pulay, P. *J. Phys. Chem.* **1995**, *99*, 3093.

(21) Scott, A. P.; Radom, L. *J. Phys. Chem.* **1996**, *100*, 16502.

(22) Wong, M. W. *Chem. Phys. Lett.* **1996**, *256*, 391.

(23) Gellini, C.; Salvi, P. R.; Vogel, E. *J. Phys. Chem. A* **2000**, *104*, 3110.

(24) Frisch, M. J.; Trucks, G. W.; Schlegel, H. B.; Scuseria, G. E.; Robb, M. A.; Cheeseman, J. R.; Zakrzewski, V. G.; J. A. Montgomery, J.; Stratmann, R. E.; Burant, J. C.; Dapprich, S.; Millam, J. M.; Daniels, A. D.; Kudin, K. N.; Strain, M. C.; Farkas, O.; Tomasi, J.; Barone, V.; Cossi, M.; Cammi, R.; Mennucci, B.; Pomelli, C.; Adamo, C.; Clifford, S.; Ochterski, J.; Petersson, G. A.; Ayala, P. Y.; Cui, Q.; Morokuma, K.; Malick, D. K.; Rabuck, A. D.; Raghavachari, K.; Foresman, J. B.; Cioslowski, J.; Ortiz, J. V.; Stefanov, B. B.; Liu, G.; Liashenko, A.; Piskorz, P.; Komaromi, I.; Gomperts, R.; Martin, R. L.; Fox, D. J.; Keith, T.; Al-Laham, M. A.; Peng, C. Y.; Nanayakkara, A.; Gonzalez, C.; Challacombe, M.; Gill, P. M. W.; Johnson, B.; Chen, W.; Wong, M. W.; Andres, J. L.; Gonzalez, C.; Head-Gordon, M.; Replogle, E. S.; Pople, J. A. *Gaussian 98*, Revision A.5; Gaussian, Inc.: Pittsburgh, PA, 1998.

(25) Raugei, S.; Cardini, G.; Schettino, V. *Mol. Phys.* **1998**, *95*, 477 and references therein.

(26) Cornell, W. D.; Cieplak, P.; Bavly, C. I.; Gould, I. R.; Merz, K. M., Jr.; Ferguson, D. M.; Spellmeyer, D. C.; Fox, T.; Caldwell, J. W.; Kollmann, P. *J. Am. Chem. Soc.* **1995**, *117*, 5179.

(27) Procacci, P.; Berne, B. J. *J. Chem. Phys.* **1994**, *101*, 2421.

(28) Hobza, P.; Selzle, H. L.; Schlag, E. W. *Chem. Rev.* **1994**, *94*, 1767.

(29) Ruoff, R. S.; Klots, T. D.; Emilsson, T.; Gutowsky, H. S. *J. Chem. Phys.* **1990**, *93*, 3142.

(30) Godfrey, P. D.; Rodgers, F. M.; Brown, R. D. *J. Am. Chem. Soc.* **1997**, *119*, 2232.